Artificial Intelligence Research and Development
I. Sanz et al. (Eds.)

doi:10.3233/FAIA230663

A Deep Learning-Based Pipeline for Computing Brain Biomarkers from MRI

Jordi MALÉ [a,1], Yann HEUZÉ [b], Juan FORTEA [c], Neus MARTÍNEZ-ABADÍAS [d] and Xavier SEVILLANO [a]

[a] *HER - Human-Environment Research Group, La Salle - Universitat Ramon Llull, Barcelona, Spain*
[b] *CNRS, Université de Bordeaux, France*
[c] *Hospital of Sant Pau, Barcelona, Spain*
[d] *Departament de Biologia Evolutiva, Ecologia i Ciències Ambientals (BEECA), Facultat de Biologia, Universitat de Barcelona (UB), Barcelona, Spain*
ORCiD ID: Jordi Malé https://orcid.org/0000-0003-4566-1921, Yann Heuzé https://orcid.org/0000-0002-0660-9613, Juan Fortea https://orcid.org/0000-0002-1340-638X, Neus Martínez-Abadías https://orcid.org/0000-0003-3061-2123, Xavier Sevillano https://orcid.org/0000-0002-6209-3033

Abstract. This ongoing work outlines a computer vision and deep learning-based pipeline to identify and detect brain biomarkers of diagnostic potential from magnetic resonance imaging (MRI) scans. In this context, this paper describes and analyses two strategies for brain landmark detection, which is a key step in brain biomarker identification: one based on a single Deep Convolutional Neural Network (DCNN) that detects multiple landmarks, and the other based on an ensemble of DCNNs trained to detect one landmark each. Based on our evaluation using two distinct datasets, our preliminary findings demonstrate that the ensemble of DCNNs achieves superior accuracy in landmarking. Specifically, it successfully detects 84% of the landmarks within a 3mm proximity to their actual locations, with an average error of less than 2mm. In contrast, a single DCNN exhibits an average error of approximately 3mm and locates only 59% of the landmarks within a 3mm distance from their true positions.

Keywords. brain landmarking, magnetic resonance imaging, deep learning

1. Introduction

The analysis of brain magnetic resonance imaging (MRI) is used for the diagnosis and prognosis of multiple genetic and developmental disorders, such as schizophrenia or Alzheimer's disease, among others. Automatic definition [1] and detection of brain landmarks [2] is crucial for this analysis, as landmark information is used for segmentation [3], registration [4] and diagnosis [5]. In this context, the obtainment of disorder-specific brain biomarkers paves the way towards personalized medicine.

[1] Corresponding Author: Jordi Malé, jordi.male@salle.url.edu.

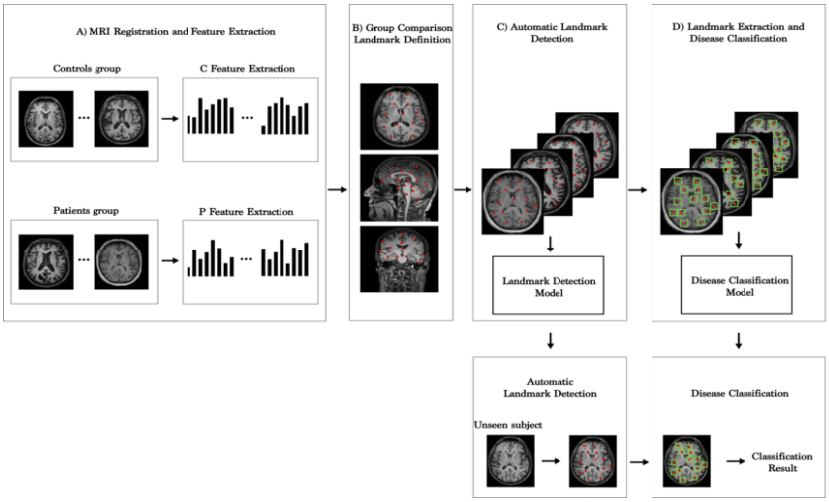

Figure 1. Proposed landmark-based disease identification framework, including (1) MRI registration and feature extraction, (2) statistical group comparison and data-driven landmark definition based on the identified discriminative voxels, (3) automatic landmark detection using DCNN, (4) landmark information extraction and (5) model-based disease classification based on the features of each input landmark

This paper presents an end-to-end pipeline –see Figure 1– that, leveraging on large datasets of brain MRI scans of healthy subjects and patients, *i)* identifies statistically significant brain anatomy differences between groups, *ii)* defines brain biomarkers of diagnostic potential based on those anatomical differences, *iii)* defines a set of brain landmarks related to the identified biomarkers, *iv)* detects those landmarks on brain MRI scans of unseen subjects, and *v)* uses the detected biomarkers to diagnose new subjects.

In the context of the proposed pipeline, the goal of this paper is to present our first results in the automatic brain landmark detection task. To that end, we trained two different Deep Convolutional Neural Network (DCNN) architectures: firstly, Multi-Landmark (ML) DCNN that predicts N landmarks, and secondly, an ensemble of N individual Single-Landmark (SL) DCNNs that predict only one landmark each.

Our preliminary results indicate that the ensemble of SL models is much more accurate than the ML model, placing landmarks with an average error below 2mm, and detecting nearly 3 times more landmarks less than 1mm away from its true location.

2. Automatic Landmark Detection

This section describes the detection of 2-dimensional landmarks on the Mid-Sagittal Plane (MSP[2]) of brain MRI scans. The ground truth coordinates of $N = 8$ landmarks (identified as diagnostic potential landmarks by our experts) were obtained by [6].

We compared two architectures of DCNN-based models: a single DCNN trained to detect the 8 landmarks, (multi-landmark model, or ML), and an ensemble of 8 DCNNs trained to detect one landmark each (single-landmark models, or SL).

[2]The MSP is the MRI slice that separates the brain into two almost-identical hemispheres.

All the DCNNs in both architectures are fed with the MSP of the brain MRI scans, and comprise: four CNN blocks (a convolutional layer, batch normalization layer, ReLU activation function, and a max-pooling layer), followed by three fully connected layers, ReLU activation functions and dropout layers to avoid overfitting. The loss function of the ML model is the average of the 8 Euclidean distances between the predicted and the ground truth landmarks. Whereas, each DCNNs in the SL model ensemble used the distance between the predicted and ground truth landmark coordinates as loss function.

3. Experimental setup

The DCNN models were trained[3] with 1837 brain MRI scans obtained from the Alzheimer's Disease Neuroimaging Initiative (ADNI-1) database. To evaluate the implemented models, we tested them with a dataset of 141 brain structural T1 MRI scans provided by Hospital Sant Pau Memory Unit (Barcelona, Spain). Different datasets were employed to evaluate the model's ability to generalize across different sources of data.

The accuracy of the landmarking results were measured in terms of: *i)* landmarking error, i.e. Euclidean distance (in mm) between the coordinates of the ground truth and the predicted landmark coordinates, and *ii)* Successful Detection Rate (SDR), defined as the percentage of predicted landmarks to be within a certain radius of their real position. We evaluated SDR at increasing radiuses from 1 to 5 mm.

4. Results, conclusions and further work

Table 1 presents the landmarking error (mean±standard deviation), SDR for the ML and SL models, and testing time (time needed to make the predictions) per image. Moreover, Figure 2b depicts the landmarking error for each specific landmark for both models.

Table 1. Landmarking error (in mm) of all landmarks for each model, and SDR of both models.

Model	Error (mm)	SDR (%)					Testing time (ms)
		1mm	2mm	3mm	4mm	5mm	
Multi-Landmark	3.03 ± 2.13	12.32	36.52	58.86	75.79	87.06	11.88
Single-Landmark	1.99 ± 1.94	29.52	66.31	83.86	90.51	93.52	92.15

As our preliminary results indicate, the ensemble of SL models outperforms the ML model both in terms of SDR and landmarking error. It is to note that the ensemble of 8 SL models places nearly 84% of the landmarks less than 3 mm away from their true location. Moreover, this higher accuracy is found for each of the 8 landmarks. This leads to the conclusion that having a model that focuses only on the loss function of the Euclidean distance of a single landmark is preferable than having a model that focuses on the average loss functions of 8 landmarks and the relative position between them.

[3] All models were implemented using PyTorch. The learning rate was initially set to 0.005 was gradually reduced to a final value of 0.0005 by applying a gamma factor of 0.95. An Adam optimizer was used with a batch size of 256. The SL models were trained for 5,000 epochs, and the ML model was trained for 10,000 epochs. All experiments were conducted on a PC with Intel Core™ i9-10980XE CPU @ 3.00GHz × 36 cores and NVIDIA GeForce RTX 2080 Ti GPU.

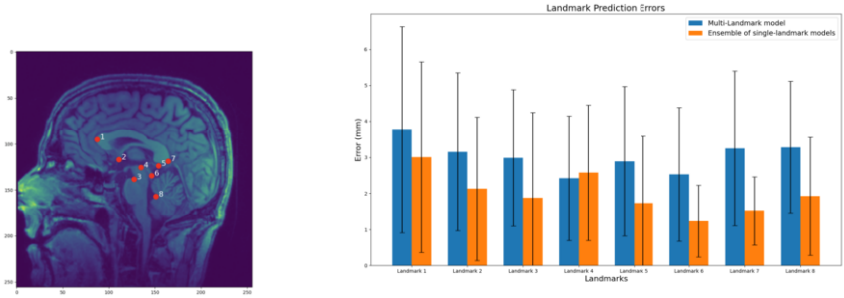

(a) (b)

Figure 2. (a) Set of N landmarks located on the MSP, and (b) Landmarking error (in mm) using the ensemble of SL models (orange bars) and the ML model (blue bars) (average value and standard deviation per landmark).

This paper has presented a deep learning-based pipeline to identify discriminative biomarkers for diagnosing psychotic disorders. A first approach to automatically detect landmarks has been implemented and validated with different datasets, obtaining promising results. Future research will include *i)* training the models using data augmentation techniques, *ii)* 3D landmarking, and *iii)* implementing the pipeline depicted in Figure 1.

Acknowledgements

This work was partly supported by Agència de Gestió d'Ajuts Universitaris i de Recerca (AGAUR) of the Generalitat de Catalunya (2021 SGR01396, 2021 SGR00706), the Spanish Ministry of Science, Innovation, and Universities under grant PID2020-113609RB-C21, the Fondation Jerome Lejeune under grant 2020b cycle-Project No.2001, and the Joan Oró grant (FI 2023) from the DRU of the Generalitat de Catalunya and the European Social Fund (2023 FI-1 00014). Data used in this work were obtained from the Alzheimer's Disease Neuroimaging Initiative (ADNI) database[4].

References

[1] Zhang J, Gao Y, Gao Y, Munsell B. Detecting Anatomical Landmarks for Fast Alzheimer's Disease Diagnosis. IEEE Transactions on Medical Imaging. 2016 06;35:1-1.

[2] Yang X, Tang WT, Tjio G, Yeo SY, Su Y. Automatic detection of anatomical landmarks in brain MR scanning using multi-task deep neural networks. Neurocomputing. 2020;396:514-21.

[3] Bokde ALWea. A new rapid landmark-based regional MRI segmentation method of the brain. Journal of the Neurological Sciences. 2002;194(1):35-40.

[4] Han D, Gao Y, Wu G, Yap PT, Shen D. Robust Anatomical Landmark Detection for MR Brain Image Registration. vol. 17; 2014. p. 186-93.

[5] Liu M, Zhang J, Adeli E. Landmark-based Deep Multi-Instance Learning for Brain Disease Diagnosis. Medical Image Analysis. 2017 10;43.

[6] Asaei A. Brain MRI landmark identification and detection; 2015. Available from: http://hdl.handle.net/20.500.12648/650.

[4]The investigators within the ADNI contributed to the design and implementation of ADNI and/or provided data but did not participate in analysis or writing of this report (see http://adni.loni.usc.edu/wp-content/uploads/how_to_apply/ADNI_Acknowledgement_List.pdf).